Double Asynchronous Orthogonal Sample Design Scheme for Probing Intermolecular Interactions

ARTICLE *in* THE JOURNAL OF PHYSICAL CHEMISTRY A · OCTOBER 2012

Impact Factor: 2.69 · DOI: 10.1021/jp300918g · Source: PubMed

THE JOURNAL OF PHYSICAL CHEMISTRY A

Article

pubs.acs.org/JPCA

Double Asynchronous Orthogonal Sample Design Scheme for Probing Intermolecular Interactions

Jing Chen,[†] Quan Bi,[†,‡] Shaoxuan Liu,[†] Xiaopei Li,[†,§] Yuhai Liu,[∥] Yanjun Zhai,[‡] Ying Zhao,[∥] Limin Yang,*[,⊥] Yizhuang Xu,*[,†] Isao Noda,[#] and Jinguang Wu[†]

[†]Beijing National Laboratory for Molecular Sciences, State Key Laboratory for Rare Earth Materials Chemistry and Applications, College of Chemistry and Molecular Engineering, and [⊥]State Key Laboratory of Nuclear Physics and Technology, Institute of Heavy Ion Physics, School of Physics, Peking University, Beijing 100871, P. R. China

[‡]College of Pharmacy, Liaoning University of Traditional Chinese Medicine, Shenyang 11660, P. R. China

[§]Institute of Process Engineering and [∥]Institute of Chemistry, Chinese Academy of Sciences, Beijing 100190, P. R. China

[#]Department of Materials Science and Engineering, University of Delaware, Newark, Delaware 19716, United States

Supporting Information

ABSTRACT: This paper introduces a new approach called double asynchronous orthogonal sample design (DAOSD) to probe intermolecular interactions. A specifically designed concentration series is selected according to the mathematical analysis to generate useful 2D correlated spectra. As a result, the interfering portions are completely removed and a pair of complementary sub-2D asynchronous spectra can be obtained. A computer simulation is applied on a model system with two solutes to study the spectral behavior of cross peaks in 2D asynchronous spectra generated by using the DAOSD approach. Variations on different spectral parameters, such as peak position, bandwidth, and absorptivity, caused by intermolecular interactions can be estimated by the characteristic spectral patterns of cross peaks in the pair of complementary sub-2D asynchronous spectra. Intermolecular interactions between benzene and iodine in CCl_4 solutions were investigated using the DAOSD approach to prove the applicability of the DAOSD method in real chemical system.

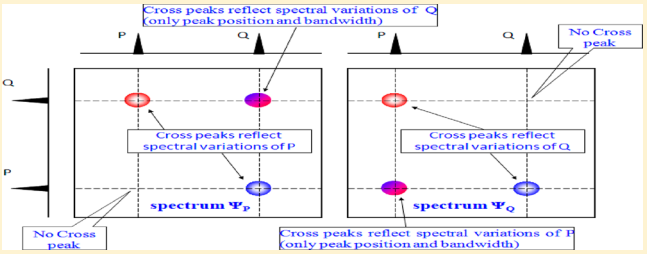

INTRODUCTION

Two-dimensional correlation spectroscopy, first proposed by Noda in the 1980s,[1,2] has been further developed[3−12] over the past two decades. The technique has attracted a great scientific interest for wide applications in characterizing a variety of chemical systems, including synthetic polymers,[13−18] proteins and peptides,[19−27] inorganic materials,[28,29] solutions and mixtures,[30−40] and many others.[41−44] One of the most attractive features in the 2D correlated spectroscopy is that the appearance of a cross peak in 2D synchronous spectra suggests the potential for investigating intermolecular interactions, which lie at the center of many physical, chemical, and biological processes.[45−51]

In our previous work, an unambiguous relationship between the cross peak in 2D synchronous spectrum and intermolecular interaction has been established by using the so-called orthogonal sample design (OSD) scheme.[32,33] The basic idea of this approach is to select suitable initial concentration series so that the resultant dynamic concentration vectors constitute a pair of orthogonal vectors and the interfering portion in cross peaks can be eliminated. Furthermore, we have refined this approach by introducing double orthogonal sample design (DOSD)[35] and asynchronous orthogonal sample design (AOSD)[36] schemes to enhance the ability to characterize spectral behaviors among solutes under intermolecular interactions.

Further studies indicate that the two-dimensional correlation spectra generated by using the OSD, DOSD, and AOSD approaches serve as a new spectral resolution enhancement method. Subtle spectral variations caused by intermolecular interactions, which are hardly observed in original one-dimensional spectra or the second derivative spectra, can be clearly visualized via the spectral patterns in two-dimensional spectra. Spectral variations on a characteristic peak of molecules involved in intermolecular interaction include changes in peak position, bandwidth, and absorptivity, which reflect molecular structural variations from different aspects. For example, variation on peak positions suggests conformation changes. Changes in absorptivities reflect the variation on dipole−dipole transition and bandwidth variation may be related to changes on molecular aggregation or hydrogen bonding. Thus, determination of the variations of peak position, bandwidth, and

Received: January 28, 2012
Revised: October 10, 2012
Published: October 11, 2012

absorptivity (increase, no changes or decrease) is important to shed light on the physical/chemical nature of intermolecular interactions. However, intermolecular interactions may render peak position, bandwidth, and/or absorptivity of characteristic peaks to change simultaneously. Consequently, the spectra patterns of 2D spectra generated by using OSD, DOSD, and AOSD approaches become too complicated to reveal how peak position, bandwidth, and absorptivity change under intermolecular interaction which prevents us from getting further information on the intermolecular interactions.

Herein, a new concept of double asynchronous orthogonal sample design (DAOSD) scheme is introduced. The 2D asynchronous spectra are decomposed into a pair of complementary sub-2D asynchronous spectra. The 2D spectra are significantly simplified and variations on peak position, bandwidth, and absorptivity can be estimated from the characteristic spectral pattern of cross peaks.

We have performed mathematical analysis, computer simulation to study the spectral behavior of cross peaks generated by using the DAOSD approach. Additionally, we applied the DAOSD approach on a real chemical system to prove the applicability of the method.

THEORY

The simulated chemical system consists of a series of solutions containing two chemical species P and Q. The characteristic peaks of P and Q are not overlapped. Variable concentrations are used as an external perturbation to construct 2D spectra. The initial concentrations of P and Q in a series of solutions (i = 1, 2, ..., n) are denoted as

$$\vec{\mathbf{C}}_{\mathrm{P}} = \begin{bmatrix} C_{\mathrm{P}}^{1(\mathrm{init})} \\ C_{\mathrm{P}}^{2(\mathrm{init})} \\ \vdots \\ C_{\mathrm{P}}^{i(\mathrm{init})} \\ \vdots \\ C_{\mathrm{P}}^{n(\mathrm{init})} \end{bmatrix} \tag{1a}$$

$$\vec{\mathbf{C}}_{\mathrm{Q}} = \begin{bmatrix} C_{\mathrm{Q}}^{1(\mathrm{init})} \\ C_{\mathrm{Q}}^{2(\mathrm{init})} \\ \vdots \\ C_{\mathrm{Q}}^{i(\mathrm{init})} \\ \vdots \\ C_{\mathrm{Q}}^{n(\mathrm{init})} \end{bmatrix} \tag{1b}$$

Under intermolecular interactions, part of P may convert into U and part of Q converts into V. This could be specified in terms of the following equilibrium and the strength of intermolecular interaction can be characterized by the corresponding equilibrium constant K.

$$\mathrm{P} + \mathrm{Q} \overset{K}{\rightleftarrows} \mathrm{U} + \mathrm{V} \tag{2}$$

Each trace of simulated 1D spectrum is the summation of the peak function of each chemical species, which is represented by a Gaussian function as shown in eq 3.

$$G^i(x) = \sum_j \varepsilon_j L C_j^{i(\mathrm{eq})} \mathrm{e}^{-\ln 2[(x-x_j)^2/w_j^2]} = \sum_j C_j^{i(\mathrm{eq})} L f_j(x) \tag{3}$$

where i is the index of the solution, j corresponds to the index of chemical species (here j stands for the four chemical species P, Q, U, V), x is wavelength, and L is the path length that is set as 1 for convenience. W_j, X_j, and ε_j are the bandwidth, peak position, and absorptivity of the characteristic band of the jth chemical species. $C_j^{i(\mathrm{eq})}$ is the equilibrium concentration of the jth chemical species in the ith solution, which can be calculated by the initial concentrations of P and Q and the equilibrium constant K. Thus, the spectral function of the ith solution should be

$$A^i(x) = C_{\mathrm{P}}^{i(\mathrm{eq})} f_{\mathrm{P}}(x) + C_{\mathrm{Q}}^{i(\mathrm{eq})} f_{\mathrm{Q}}(x) + C_{\mathrm{U}}^{i(\mathrm{eq})} f_{\mathrm{U}}(x) + C_{\mathrm{V}}^{i(\mathrm{eq})} f_{\mathrm{V}}(x) \tag{4}$$

Because

$$C_{\mathrm{P}}^{i(\mathrm{eq})} = C_{\mathrm{P}}^{i(\mathrm{init})} - C_{\mathrm{U}}^{i(\mathrm{eq})} \tag{5a}$$

$$C_{\mathrm{Q}}^{i(\mathrm{eq})} = C_{\mathrm{Q}}^{i(\mathrm{init})} - C_{\mathrm{V}}^{i(\mathrm{eq})} \tag{5b}$$

eq 4 can be expressed by eq 6.

$$A^i(x) = C_{\mathrm{P}}^{i(\mathrm{init})} f_{\mathrm{P}}(x) + C_{\mathrm{Q}}^{i(\mathrm{init})} f_{\mathrm{Q}}(x) + C_{\mathrm{U}}^{i(\mathrm{eq})} [f_{\mathrm{U}}(x) - f_{\mathrm{P}}(x)] + C_{\mathrm{V}}^{i(\mathrm{eq})} [f_{\mathrm{V}}(x) - f_{\mathrm{Q}}(x)] \tag{6}$$

After the average value at each wavelength is removed, dynamic intensity can be obtained per eq 7.

$$\tilde{A}^i(x) = \tilde{C}_{\mathrm{P}}^i f_{\mathrm{P}}(x) + \tilde{C}_{\mathrm{Q}}^i f_{\mathrm{Q}}(x) + \tilde{C}_{\mathrm{U}}^i [f_{\mathrm{U}}(x) - f_{\mathrm{P}}(x)] + \tilde{C}_{\mathrm{V}}^i [f_{\mathrm{V}}(x) - f_{\mathrm{Q}}(x)] \tag{7}$$

where $\tilde{C}_{\mathrm{P}}$, $\tilde{C}_{\mathrm{Q}}$, $\tilde{C}_{\mathrm{U}}$, and $\tilde{C}_{\mathrm{V}}$ are dynamic concentrations of P, Q, U, and V.

$$\tilde{C}_{\mathrm{P}}^i = C_{\mathrm{P}}^{i(\mathrm{init})} - C_{\mathrm{P}}^{i(\mathrm{av})} \tag{8a}$$

$$\tilde{C}_{\mathrm{U}}^i = C_{\mathrm{U}}^{i(\mathrm{eq})} - C_{\mathrm{U}}^{\mathrm{eq(av)}} \tag{8b}$$

$$\tilde{C}_{\mathrm{Q}}^i = C_{\mathrm{Q}}^{i(\mathrm{init})} - C_{\mathrm{Q}}^{i(\mathrm{av})} \tag{8c}$$

$$\tilde{C}_{\mathrm{V}}^i = C_{\mathrm{V}}^{i(\mathrm{eq})} - C_{\mathrm{V}}^{\mathrm{eq(av)}} \tag{8d}$$

The corresponding asynchronous spectrum can be calculated according to eq 9:[4]

$$\Psi(x,y) = \frac{1}{n-1} \vec{\tilde{\mathbf{A}}}^{\mathrm{T}}(x) \mathbf{N} \vec{\tilde{\mathbf{A}}}(y) \tag{9}$$

where T stands for transposition, n is the number of solutions used to construct the 2D asynchronous spectrum, and $\mathbf{N}$ is the Hilbert–Noda transformation matrix.

After eq 9 is combined with eq 7, the corresponding asynchronous spectrum is as shown in eq 10.

$$\Psi(x,y) = \sum_{i=1}^{16} R_i(x,y) \tag{10}$$

dx.doi.org/10.1021/jp300918g | J. Phys. Chem. A 2012, 116, 10904–10916

where

$$R_1(x,y) = f_P(x) f_P(y) \vec{\tilde{C}}_P^T \mathbf{N} \vec{\tilde{C}}_P$$

$$R_2(x,y) = f_Q(x) f_Q(y) \vec{\tilde{C}}_Q^T \mathbf{N} \vec{\tilde{C}}_Q$$

$$R_3(x,y) = f_P(x) f_Q(y) \vec{\tilde{C}}_P^T \mathbf{N} \vec{\tilde{C}}_Q$$

$$R_4(x,y) = f_Q(x) f_P(y) \vec{\tilde{C}}_Q^T \mathbf{N} \vec{\tilde{C}}_P$$

$$R_5(x,y) = f_P(x)[f_U(y) - f_P(y)] \vec{\tilde{C}}_P^T \mathbf{N} \vec{\tilde{C}}_U$$

$$R_6(x,y) = f_P(x)[f_V(y) - f_Q(y)] \vec{\tilde{C}}_P^T \mathbf{N} \vec{\tilde{C}}_V$$

$$R_7(x,y) = f_Q(x)[f_U(y) - f_P(y)] \vec{\tilde{C}}_Q^T \mathbf{N} \vec{\tilde{C}}_U$$

$$R_8(x,y) = f_Q(x)[f_V(y) - f_Q(y)] \vec{\tilde{C}}_Q^T \mathbf{N} \vec{\tilde{C}}_V$$

$$R_9(x,y) = [f_U(x) - f_P(x)] f_P(y) \vec{\tilde{C}}_U^T \mathbf{N} \vec{\tilde{C}}_P$$

$$R_{10}(x,y) = [f_U(x) - f_P(x)] f_Q(y) \vec{\tilde{C}}_U^T \mathbf{N} \vec{\tilde{C}}_Q$$

$$R_{11}(x,y) = [f_V(x) - f_Q(x)] f_P(y) \vec{\tilde{C}}_V^T \mathbf{N} \vec{\tilde{C}}_P$$

$$R_{12}(x,y) = [f_V(x) - f_Q(x)] f_Q(y) \vec{\tilde{C}}_V^T \mathbf{N} \vec{\tilde{C}}_Q$$

$$R_{13}(x,y) = [f_U(x) - f_P(x)][f_U(y) - f_P(y)] \vec{\tilde{C}}_U^T \mathbf{N} \vec{\tilde{C}}_U$$

$$R_{14}(x,y) = [f_V(x) - f_Q(x)][f_V(y) - f_Q(y)] \vec{\tilde{C}}_V^T \mathbf{N} \vec{\tilde{C}}_V$$

$$R_{15}(x,y) = [f_V(x) - f_Q(x)][f_U(y) - f_P(y)] \vec{\tilde{C}}_V^T \mathbf{N} \vec{\tilde{C}}_U$$

$$R_{16}(x,y) = [f_U(x) - f_P(x)][f_V(y) - f_Q(y)] \vec{\tilde{C}}_U^T \mathbf{N} \vec{\tilde{C}}_V \quad (11)$$

$R_1(x,y)$, $R_2(x,y)$, $R_3(x,y)$, and $R_4(x,y)$ are interference parts and have to be removed.

Because the Hilbert−Noda matrix possesses the following two basic properties as shown in eqs 12 and 13,

$$\vec{\mathbf{A}}^T \mathbf{N} \vec{\mathbf{A}} = 0 \quad (12)$$

$$\vec{\mathbf{A}}^T \mathbf{N} \vec{\mathbf{B}} = -\vec{\mathbf{B}}^T \mathbf{N} \vec{\mathbf{A}} \quad (13)$$

$R_1(x,y)$ and $R_2(x,y)$ are zero and can be naturally removed. To remove $R_3(x,y)$ and $R_4(x,y)$, a suitable initial concentration series of P and Q is adopted so that the corresponding dynamic concentration vectors of P and Q satisfy eq 14.

$$\vec{\tilde{C}}_P^T \mathbf{N} \vec{\tilde{C}}_Q = -\vec{\tilde{C}}_Q^T \mathbf{N} \vec{\tilde{C}}_P = 0 \quad (14)$$

Our approach is that two groups of solutions are prepared. Each group is composed of n solutions. The initial concentrations of P and Q in the two groups are listed in eq 15.

Group 1

$$\vec{C}_Q = \begin{bmatrix} s \\ \vdots \\ s \\ \vdots \\ s \end{bmatrix}$$

$$\vec{C}_Q = \begin{bmatrix} C_Q^1 \\ \vdots \\ C_Q^i \\ \vdots \\ C_Q^n \end{bmatrix} \quad (15a)$$

Group 2

$$\vec{C}_P = \begin{bmatrix} C_P^1 \\ \vdots \\ C_P^i \\ \vdots \\ C_P^n \end{bmatrix}$$

$$\vec{C}_Q = \begin{bmatrix} t \\ \vdots \\ t \\ \vdots \\ t \end{bmatrix} \quad (15b)$$

where s and t are constant values that are set arbitrarily.

For any $i, j \in \{1, ..., n\}$, if $i \neq j$,

$$C_P{}^i \neq C_P{}^j \qquad C_Q{}^i \neq C_Q{}^j$$

Table 1. Spectral Parameters of P and Q in the Model System

spectral variable	peak position (cm^{-1})	bandwidth (cm^{-1})	absorptivity
P	150	20	1.0
Q	350	20	1.0

Table 2. Initial Concentrations of P and Q in the Model System, which Meet the Requirement of the DAOSD Approach

index of the solutions	C_P (arbitrary unit)	C_Q (arbitrary unit)
	Group 1	
1	12.00	12.00
2	12.00	10.00
3	12.00	8.00
4	12.00	0.00
	Group 2	
1	12.00	8.00
2	10.00	8.00
3	6.00	8.00
4	0.00	8.00

dx.doi.org/10.1021/jp300918g | J. Phys. Chem. A 2012, 116, 10904−10916

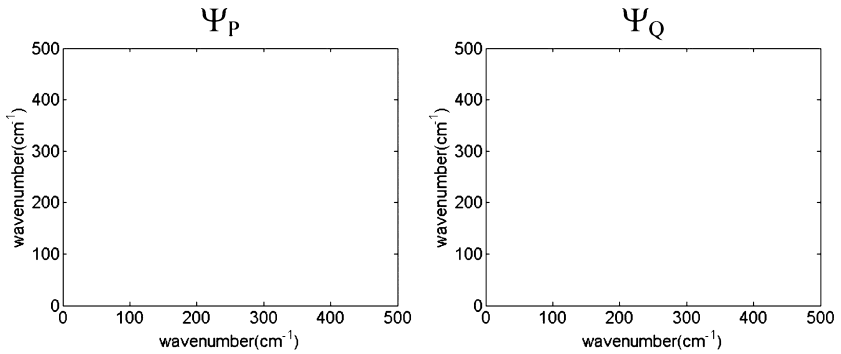

Figure 1. Simulated 2D spectra of the model system without intermolecular interactions (K = 0).

The asynchronous spectra constructed on the basis of the 1D spectra of the solutions from Group 1 and Group 2 are denoted as $\Psi_P(x,y)$ and $\Psi_Q(x,y)$, respectively. According to eq 15a, the dynamic concentration of P is zero in the solutions of Group 1. Thus, $R_3(x,y)$ and $R_4(x,y)$ in eq 11 become zero, thereby removing the interfering parts from $\Psi_P(x,y)$. Similarly, $R_3(x,y)$ and $R_4(x,y)$ in $\Psi_Q(x,y)$ are also removed because the dynamic concentration of Q is zero in the solutions of Group 2. Therefore, both $\Psi_P(x,y)$ and $\Psi_Q(x,y)$ can reflect the effect of intermolecular interactions between P and Q without the undesirable interference portion arising from the dominant background effect of concentration. $\Psi_P(x,y)$ and $\Psi_Q(x,y)$ can be further simplified according to the basic mathematic properties of the Hilbert–Noda matrix: (1) On the basis of eq 12, $R_{13}(x,y)$ and $R_{14}(x,y)$ in eq 11 are zero for both $\Psi_P(x,y)$ and $\Psi_Q(x,y)$. (2) According to the reaction listed in eq 2,

$$\vec{\tilde{C}}_U = \vec{\tilde{C}}_V \tag{16}$$

Scheme 1. Schematic Diagram of the 2D Asynchronous Spectra, Where the Contour Map Is Divided into Four Spectral Domains

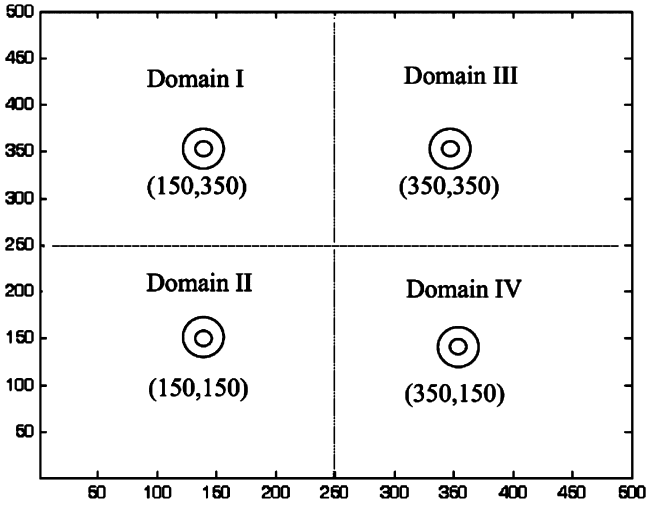

Table 3. Spectral Parameters of P, Q, U, and V in the Model System Where the Absorptivity, Peak Position, and Bandwidth of V Are Variable

spectral variable	peak position (cm^{-1})	bandwidth (cm^{-1})	absorptivity
P	150	20	1.0
Q	350	20	1.0
U	150	20	1.0
V	X_V	W_V	ε_V

Scheme 2. Schematic Diagram of the Spectral Properties of the 2D Asynchronous Spectra Generated by the DAOSD Approach

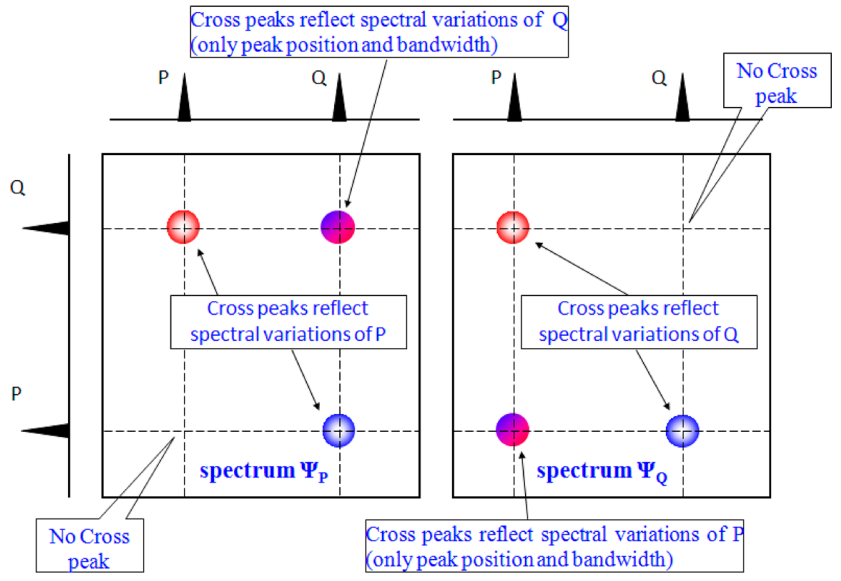

dx.doi.org/10.1021/jp300918g | J. Phys. Chem. A 2012, 116, 10904–10916

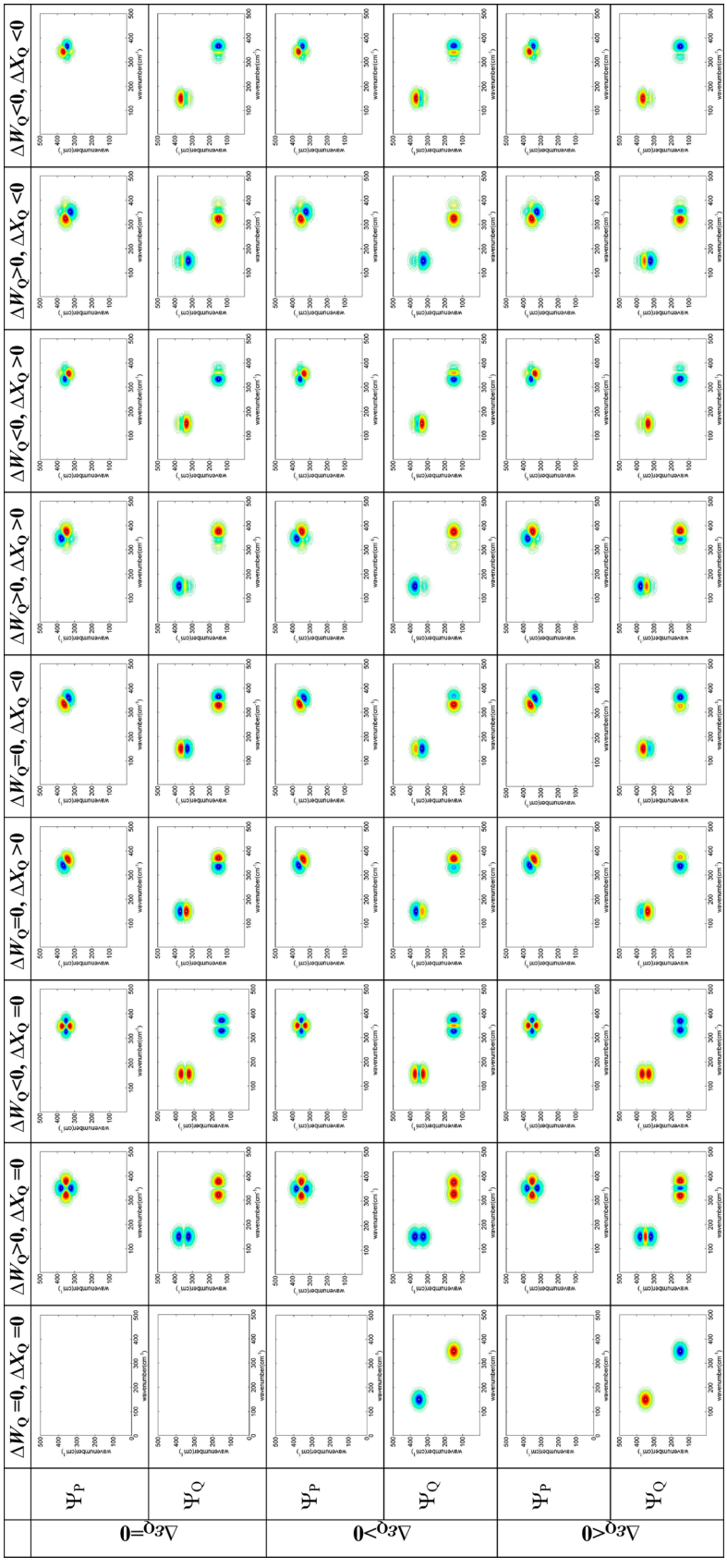

Figure 2. 2D asynchronous spectra of the model system when $\Delta\varepsilon_{QJ}$ ΔW_{QJ} and ΔX_{QJ} change.

dx.doi.org/10.1021/jp300918g | J. Phys. Chem. A 2012, 116, 10904−10916

Thus, $R_{15}(x,y)$ and $R_{16}(x,y)$ in eq 11 are zero in $\Psi_P(x,y)$ and $\Psi_Q(x,y)$.

Because of the specifically designed initial concentration series of P and Q, both $\Psi_P(x,y)$ and $\Psi_Q(x,y)$ can be further simplified as follows: According to eq 15a, the dynamic concentrations of P are zero. Thus, $R_5(x,y)$, $R_6(x,y)$, $R_9(x,y)$, and $R_{11}(x,y)$ in eq 11 are zero. The resultant $\Psi_P(x,y)$ is simplified as

$$\Psi_P(x,y) = R_7(x,y) + R_8(x,y) + R_{10}(x,y) + R_{12}(x,y) \tag{17a}$$

Similarly, the dynamic concentrations of Q are zero on the basis of eq 15b. Thus, $R_7(x,y)$, $R_8(x,y)$, $R_{10}(x,y)$, and $R_{12}(x,y)$ in eq 10 are zero. The corresponding $\Psi_Q(x,y)$ can be expressed as

$$\Psi_Q(x,y) = R_5(x,y) + R_6(x,y) + R_9(x,y) + R_{11}(x,y) \tag{17b}$$

EXPERIMENTAL SECTION

1. Model System. The simulated one-dimensional spectrum for each solution with designed concentrations of different chemical species was generated by using a program written in our lab. Two-dimensional asynchronous spectra in simulation study and the following real chemical system were calculated by using the software of MATLAB (The Math Works Inc.). In each asynchronous spectrum, red means the sign of the spectrum is positive, whereas blue means negative.

2. Real Chemical System. Iodine and benzene, both AR grade, were purchased from Beijing Chemical Reagent Co. (Beijing, China). CCl_4, AR grade, was ordered from Xilong Chemical Co., Ltd. (Guangxi, China).

FT-IR spectra were measured on a Thermo-Fischer Nicolet 6700 spectrometer using a BaF_2 cell with a fixed spacing (100 μm). All spectra were obtained at a resolution of 0.5 cm^{-1} and 32 scans were coadded.

UV−Vis spectra for the solutions were recorded on a Perkin-Elmer Lambda 35 spectrometer in 1 mm absorption cell.

RESULTS AND DISCUSSION

1. Role of DAOSD in Eliminating the Interfering Portion from 2D Asynchronous Spectra. First, we simulate a chemical system where no intermolecular interaction occurs between P and Q, which could be achieved by setting the equilibrium constant K as zero. Thus, U and V do not occur in the solutions. Spectral features of the characteristic bands for P and Q, including bandwidths (W_P and W_Q), peak positions (X_P and X_Q), and absorptivities (ε_P and ε_Q) are set as listed in Table 1. Initial concentrations of P and Q (Table 2) meet the requirement of the DAOSD approach. No cross peak occurs in either $\Psi_P(x,y)$ or $\Psi_Q(x,y)$ (Figure 1). Thus, $\Psi_P(x,y)$ and $\Psi_Q(x,y)$ are free from interference portion that has nothing to do with intermolecular interaction between P and Q.

2. Basic Properties of Asynchronous Spectra Generated by Using DAOSD Approach. The asynchronous spectrum is composed of four spectral domains, as shown in Scheme 1. The basic properties of the cross peaks in different spectral region are summarized as follows.

a. Domain II of $\Psi_P(x,y)$ and Domain III of $\Psi_Q(x,y)$. On the basis of the assumption that the characteristic peaks of P, U and Q, V do not overlap, we have

Table 4. Spectral Parameters of P, Q, U, and V in the Model System Where the Absorptivity, Peak Position, and Bandwidth of U Are Variable

spectral variable	peak position (cm^{-1})	bandwidth (cm^{-1})	absorptivity
P	150	20	1.0
Q	350	20	1.0
U	X_U	W_U	ε_U
V	350	20	1.0

$$f_Q(x) = 0, \quad f_V(x) = 0, \quad \text{as} \quad x \in [0, 250)$$
$$f_Q(y) = 0, \quad f_V(y) = 0, \quad \text{as} \quad y \in [0, 250) \tag{19a}$$

$$f_P(x) = 0, \quad f_U(x) = 0, \quad \text{as} \quad x \in [250, 500]$$
$$f_P(y) = 0, \quad f_U(y) = 0, \quad \text{as} \quad y \in [250, 500] \tag{19b}$$

As a result, $R_7(x,y)$, $R_8(x,y)$, $R_{10}(x,y)$, and $R_{12}(x,y)$ in eq 11 are zero in the spectral domain II of $\Psi_P(x,y)$. Therefore

$$\Psi_P(x,y) = R_7(x,y) + R_8(x,y) + R_{10}(x,y) + R_{12}(x,y) = 0$$

In the spectral domain III of $\Psi_Q(x,y)$ we have similar results:

$$\Psi_Q(x,y) = R_5(x,y) + R_6(x,y) + R_9(x,y) + R_{11}(x,y) = 0$$

Thus, no cross peak appears in either domain II of $\Psi_P(x,y)$ or domain III of $\Psi_Q(x,y)$.

b. Domain III of $\Psi_P(x,y)$ and Domain II of $\Psi_Q(x,y)$. $R_7(x,y)$ and $R_{10}(x,y)$ in eq 11 are zero in the spectral domain III of $\Psi_P(x,y)$. Thus,

$$\Psi_P(x,y) = R_8(x,y) + R_{12}(x,y) \tag{20}$$

According to eq 3, f_j can be expressed as eq 21.

$$f_j(x) = \varepsilon_j e^{-\ln 2[(x-X_j)^2/W_j^2]} = \varepsilon_j g_j(x) \tag{21}$$

where $g_j(x)$ is the function of peak position and bandwidth:

$$g_j(x) = e^{-\ln 2[(x-X_j)^2/W_j^2]}$$

After combining eq 21 with eq 11 and eq 20, we have

$$\Psi_P(x,y) = \varepsilon_Q \varepsilon_V [g_Q(x)\, g_V(y) - g_Q(y)\, g_V(x)] \vec{\tilde{C}}_Q^{\,T} \mathbf{N} \vec{\tilde{C}}_V \tag{22a}$$

Similarly, the cross peaks in domain II of $\Psi_Q(x,y)$ can be expressed as follows:

$$\Psi_Q(x,y) = \varepsilon_P \varepsilon_U [g_P(x)\, g_U(y) - g_P(y)\, g_U(x)] \vec{\tilde{C}}_P^{\,T} \mathbf{N} \vec{\tilde{C}}_U \tag{22b}$$

Therefore, the spectral patterns of cross peaks in domain III of $\Psi_P(x,y)$ and those in domain II of $\Psi_Q(x,y)$ reflect the variation of peak position/bandwidth of the Q band and peak position/bandwidth of the P band, respectively.

c. Domain I of $\Psi_P(x,y)$ and Domain IV of $\Psi_Q(x,y)$. Because cross peaks in domain I and domain IV of $\Psi_P(x,y)$ and $\Psi_Q(x,y)$ are antisymmetric about the diagonal, only the cross peaks in domain I of $\Psi_P(x,y)$ and domain IV of $\Psi_Q(x,y)$ are discussed.

In domain I, $x \in [0, 250)$, $y \in [250, 500)$. Thus, $R_7(x,y)$, $R_8(x,y)$, and $R_{12}(x,y)$ in eq 11 are zero and the cross peaks change into

$$\Psi_P(x,y) = R_{10}(x,y)$$

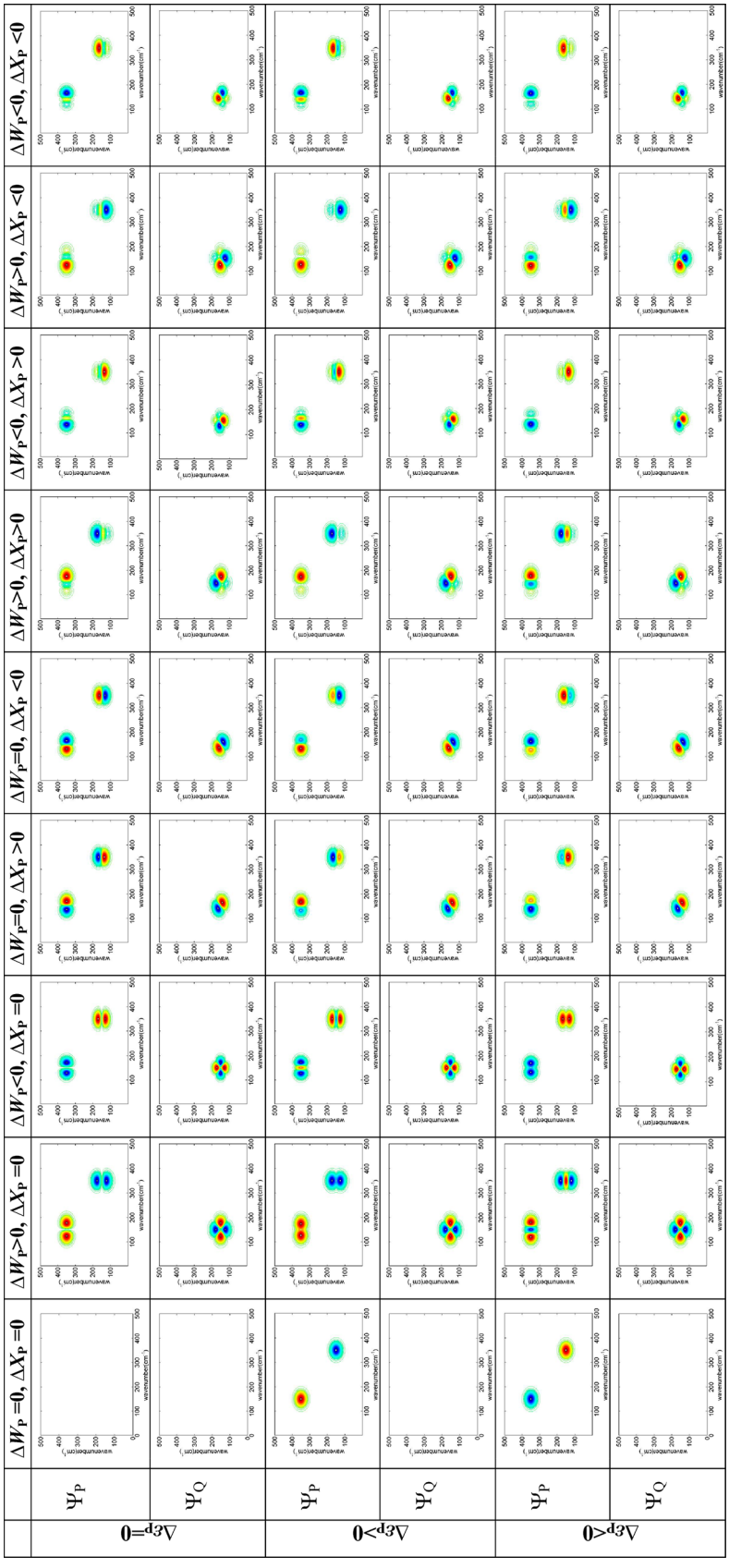

Figure 3. 2D asynchronous spectra of the model system when $\Delta\varepsilon_P$, ΔW_P, and ΔX_P change.

dx.doi.org/10.1021/jp300918g | J. Phys. Chem. A 2012, 116, 10904−10916

After combination of eq 21 and eq 11, we have

$$\begin{aligned}\Psi_P(x,y) &= [\varepsilon_U g_U(x) - \varepsilon_P g_P(x)]\varepsilon_Q g_Q(y)\vec{\tilde{C}}_U^T \mathbf{N}\vec{\tilde{C}}_Q \\ &= [\varepsilon_U g_U(x) - \varepsilon_U g_P(x) - \varepsilon_P g_P(x) + \varepsilon_U g_P(x)] \\ &\quad \varepsilon_Q g_Q(y)\vec{\tilde{C}}_U^T \mathbf{N}\vec{\tilde{C}}_Q \\ &= \varepsilon_Q \varepsilon_U [g_U(x) - g_P(x)] g_Q(y)\vec{\tilde{C}}_U^T \mathbf{N} \\ &\quad \vec{\tilde{C}}_Q + \varepsilon_Q(\varepsilon_U - \varepsilon_P) g_P(x)\, g_Q(y)\vec{\tilde{C}}_U^T \mathbf{N}\vec{\tilde{C}}_Q \end{aligned} \quad (23a)$$

Therefore, the cross peaks in domain I of $\Psi_P(x,y)$ are composed of two parts: the first term reflects the variations of bandwidth and peak position of the P band; the second term reveals the variation of absorptivity of characteristic peak of the P band.

Similarly, the cross peaks in domain IV of $\Psi_Q(x,y)$ are expressed as

$$\begin{aligned}\Psi_Q(x,y) &= \varepsilon_P \varepsilon_V [g_V(x) - g_Q(x)] g_P(y)\vec{\tilde{C}}_V^T \mathbf{N} \\ &\quad \vec{\tilde{C}}_P + \varepsilon_P(\varepsilon_V - \varepsilon_Q) g_Q(x)\, g_P(y)\vec{\tilde{C}}_V^T \mathbf{N}\vec{\tilde{C}}_P \end{aligned} \quad (23b)$$

That is to say, cross peaks in domain IV of $\Psi_Q(x,y)$ are composed of the portion reflecting variations of peak position and bandwidth of the Q band and the portion that is related to the variation of absorptivity of the Q band.

The advantage of the DAOSD approach can be manifested by cross peaks in domain I and domain IV. In 2D spectra generated by using OSD, AOSD, and DOSD approaches, cross peaks in domain I and domain IV of 2D spectra are related to the spectral variations of both P and Q. When peak position, bandwidth, and absorptivity of the characteristic bands of P and Q change simultaneously, the resultant spectral pattern becomes too complicated to reveal spectral variations in detail. In the DAOSD approach, cross peaks in domain I of $\Psi_P(x,y)$ reflect variations of the P band whereas cross peaks in domain IV of $\Psi_Q(x,y)$ reveal changes of the Q band (Scheme 2). Thus, it becomes possible to study the variations of peak position, bandwidth, and absorptivity under intermolecular interactions separately via a pair of asynchronous 2D spectra.

According to eq 23a and eq 23b, the cross peaks in domain I and domain IV can be decomposed into contributions related to variation of absorptivity and contribution relevant to variations of peak position and bandwidth. On the other hand, information related to variations of peak position and bandwidth band can be deduced from spectral patterns in domain III of $\Psi_P(x,y)$ and those in domain II of $\Psi_Q(x,y)$. Therefore, combination of cross peaks in domain III of $\Psi_P(x,y)$ and those in domain II of $\Psi_Q(x,y)$ as well as cross peaks in domain I and IV, the variation of absorptivity can also be determined.

3. Basic Spectral Patterns in Asynchronous Spectra. Here we examined the behaviors of the cross peaks in asynchronous spectra generated by using the DAOSD approach as a consequence of the variations of spectral parameters of P and Q. There are six variables: $\Delta\varepsilon_P$, ΔW_P, ΔX_P, $\Delta\varepsilon_Q$, ΔW_Q, and ΔX_Q, where

Table 5. Spectral Parameters of P, Q, U, and V in the Model System Where the Absorptivity of U and V Are Variable

spectral variable	peak position (cm^{-1})	bandwidth (cm^{-1})	absorptivity
P	150	20	1.0
Q	350	20	1.0
U	150	20	ε_U
V	350	20	ε_V

$$\Delta\varepsilon_P = \varepsilon_U - \varepsilon_P, \quad \Delta W_P = W_U - W_P, \quad \Delta X_P = X_U - X_P$$
$$\Delta\varepsilon_Q = \varepsilon_V - \varepsilon_Q, \quad \Delta W_Q = W_V - W_Q, \quad \Delta X_Q = X_V - X_Q$$

Each variable occurs in three states: increase, invariant, and decrease. Thus, there are $3^6 = 729$ possible situations. It will be a tedious work to exhaust each of the 729 possible situations. Fortunately, cross peaks caused by the variations of spectral parameters of P and Q due to intermolecular interactions are manifested in separated regions in $\Psi_P(x,y)$ and $\Psi_Q(x,y)$. That is to say, the relationship between spectral patterns and $\Delta\varepsilon_P$, ΔW_P, and ΔX_P is independent of the relationship between spectral patterns and $\Delta\varepsilon_Q$, ΔW_Q, and ΔX_Q. Herein, the relationships between spectral patterns and $\Delta\varepsilon_Q$, ΔW_Q, and ΔX_Q as well as the relationships between spectral patterns and $\Delta\varepsilon_P$, ΔW_P, and ΔX_P are investigated separately.

a. Relationship between Spectral Patterns and $\Delta\varepsilon_Q$, ΔW_Q, and ΔX_Q. First, we examined the behaviors of the cross peaks in asynchronous spectra generated by using the DAOSD approach as a consequence of the variations of spectral parameters of Q whereas the spectral parameters of U are the same as those of P. The initial concentrations of P and Q are listed in Table 2 and the spectral parameters for P, Q, U, and V used for the simulation are summarized in Table 3. The equilibrium constant K is set as 0.01. In this case, there are three variables: $\Delta\varepsilon_Q$, ΔW_Q, and ΔX_Q. Thus, the number of possible situations is $3^3 = 27$. The corresponding spectra are shown in Figure 2. The states of $\Delta\varepsilon_Q$, ΔW_Q, and ΔX_Q can be estimated via the spectral patterns in $\Psi_P(x,y)$ and $\Psi_Q(x,y)$ (the properties of the patterns are discussed comprehensively in the Supporting Information).

b. Relationship between Spectral Patterns and $\Delta\varepsilon_P$, ΔW_P, and ΔX_P. The patterns in domain I of $\Psi_P(x,y)$ and domain II of $\Psi_Q(x,y)$ reflect the spectral variations of P. The initial concentrations of P and Q are listed in Table 2, and the spectral parameters for P, Q, U, and V used for the simulation are summarized in Table 4. The calculated spectral patterns are listed in Figure 3. Similarly, the state of $\Delta\varepsilon_P$, ΔW_P, and ΔX_P can be estimated via the spectral patterns in $\Psi_P(x,y)$ and $\Psi_Q(x,y)$.

When the signs of $\Delta\varepsilon_P$, ΔW_P, ΔX_P, $\Delta\varepsilon_Q$, ΔW_Q, and ΔX_Q are concerned, there are $3^6 = 729$ possible situations. In the DAOSD approach, variations of $\Delta\varepsilon_Q$, ΔW_Q, and ΔX_Q are manifested by cross peaks in domain III of $\Psi_P(x,y)$ and domain IV of $\Psi_Q(x,y)$, whereas variations of $\Delta\varepsilon_P$, ΔW_P, and ΔX_P are reflected by cross peaks in domain II of $\Psi_Q(x,y)$ and domain I of $\Psi_P(x,y)$. As a result, each of the 729 possible situations of $\Delta\varepsilon_P$, ΔW_P, ΔX_P, $\Delta\varepsilon_Q$, ΔW_Q, and ΔX_Q can be reflected by the combination of one of the pattern shown in Figure 2 and one of the pattern shown in Figure 3.

Therefore, the states of $\Delta\varepsilon_P$, ΔW_P, ΔX_P, $\Delta\varepsilon_Q$, ΔW_Q, and ΔX_Q can be estimated via spectral patterns in $\Psi_P(x,y)$ and $\Psi_Q(x,y)$ by using the DAOSD approach.

dx.doi.org/10.1021/jp300918g | J. Phys. Chem. A 2012, 116, 10904−10916

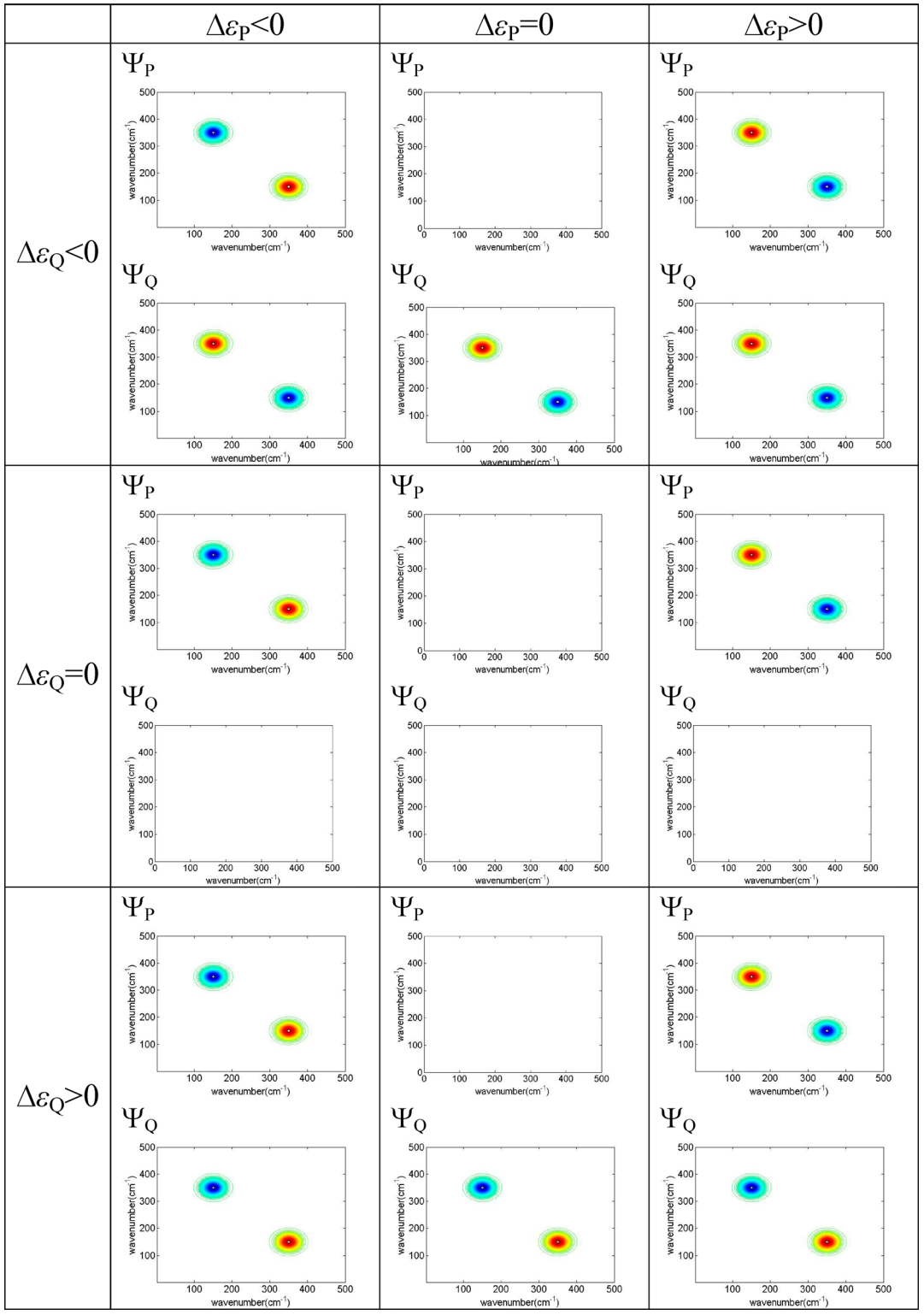

Figure 4. 2D asynchronous spectra of the model system when $\Delta\varepsilon_P$ and $\Delta\varepsilon_Q$ change.

4. Ability of the DAOSD Approach on the Analysis of Complex Spectral Variations Caused by Intermolecular Interactions. In the DAOSD approach, variations of the characteristic peaks of P and Q are manifested in separated spectral regions in both $\Psi_P(x,y)$ and $\Psi_Q(x,y)$. Therefore, it is much easier to analyze complex spectral variations caused by intermolecular interactions. Here we use two typical examples to show how we can use $\Psi_P(x,y)$ and $\Psi_Q(x,y)$ to analyze the complex spectral variations of P and Q under intermolecular interactions.

a. Variations in Absorptivities of P and Q. According to our previous work, the determination of the signs of $\Delta\varepsilon_P$ and $\Delta\varepsilon_Q$ is a challenging task. $\Delta\varepsilon_P$ and $\Delta\varepsilon_Q$ occur in three states: increase, invariant, and decrease. Thus, there are nine combinatory possible states. The variation of $\Delta\varepsilon_P$ or $\Delta\varepsilon_Q$ can only be reflected by a single peak in domain I/IV of 2D correlated

dx.doi.org/10.1021/jp300918g | J. Phys. Chem. A 2012, 116, 10904−10916

Table 6. Relationship between the Signs of Cross Peaks in Asynchronous $\Psi_P(x,y)$ and $\Psi_Q(x,y)$ and the Corresponding $\Delta\varepsilon_P$ and $\Delta\varepsilon_Q$

index	sign of the cross peak in domain I of spectrum Ψ_P	sign of the cross peak in domain IV of spectrum Ψ_Q	corresponding $\Delta\varepsilon_P$ and $\Delta\varepsilon_Q$
1	blank	blank	$\Delta\varepsilon_P = 0$, $\Delta\varepsilon_Q = 0$
2	blank	positive	$\Delta\varepsilon_P = 0$, $\Delta\varepsilon_Q > 0$
3	blank	negative	$\Delta\varepsilon_P = 0$, $\Delta\varepsilon_Q < 0$
4	positive	blank	$\Delta\varepsilon_P > 0$, $\Delta\varepsilon_Q = 0$
5	positive	positive	$\Delta\varepsilon_P > 0$, $\Delta\varepsilon_Q > 0$
6	positive	negative	$\Delta\varepsilon_P > 0$, $\Delta\varepsilon_Q < 0$
7	negative	blank	$\Delta\varepsilon_P < 0$, $\Delta\varepsilon_Q = 0$
8	negative	positive	$\Delta\varepsilon_P < 0$, $\Delta\varepsilon_Q > 0$
9	negative	negative	$\Delta\varepsilon_P < 0$, $\Delta\varepsilon_Q < 0$

spectra generated by using the OSD, AOSD, and DOSD approaches. Moreover, the sign of the cross peak is under the influence of both $\Delta\varepsilon_P$ and $\Delta\varepsilon_Q$. Consequently, it is impossible to determine the signs of both $\Delta\varepsilon_P$ and $\Delta\varepsilon_Q$ simultaneously even if the DOSD approach is used.[33]

In the DAOSD approach, $\Delta\varepsilon_P$ is reflected by a single cross peak in domain I of $\Psi_P(x,y)$ whereas $\Delta\varepsilon_Q$ is manifested by a single cross peak in the domain IV of $\Psi_Q(x,y)$. As a result, there are three states in domain I of $\Psi_P(x,y)$: positive peak, no peak, negative peak. Similarly, positive peak, no peak and negative peak appear in domain IV of $\Psi_Q(x,y)$. Thus, nine types of combined spectral patterns from $\Psi_P(x,y)$ and $\Psi_Q(x,y)$ can be generated. That is to say, the number of spectral patterns is enough to reflect the nine combinatory possible variations of $\Delta\varepsilon_P$ and $\Delta\varepsilon_Q$. The spectral parameters for P, Q, U, and V used for the simulation are summarized in Table 5. The initial concentrations of P and Q are listed in Table 2. As shown in Figure 4 and Table 6, a one-to-one corresponding between the signs of $\Delta\varepsilon_P$ and $\Delta\varepsilon_Q$ and the spectral patterns in nondiagonal domains of both $\Psi_P(x,y)$ and $\Psi_Q(x,y)$ can be established. That is to say, the DAOSD approach manages to determine the signs of both $\Delta\varepsilon_P$ and $\Delta\varepsilon_Q$ simultaneously.

b. Analysis of Complex Spectral Variations by Using the DAOSD Approach. Here, we simulate a situation where intermolecular interactions bring about complex spectral variations. The initial concentrations that meet the requirement of the DAOSD are listed in Table 2. The corresponding $\Psi_P(x,y)$ and $\Psi_Q(x,y)$ are plotted in Figure 5. The patterns of $\Psi_P(x,y)$ and $\Psi_Q(x,y)$ provide enough information to deduce spectral variations. The pattern in domain III of $\Psi_P(x,y)$ exhibits a diamond shape and the horizontal peaks are positive, demonstrating that $\Delta W_Q > 0$ and $\Delta X_Q = 0$. A pair of cross peaks that are antisymmetric about the diagonal line occur in domain II of the $\Psi_Q(x,y)$ and the bottom-right peak is positive, which illustrates that $\Delta X_P > 0$ and $\Delta W_P = 0$. There are three peaks in domain IV of the $\Psi_Q(x,y)$. Two positive peaks sandwich a negative peak. The sign of cross peak at (350, 150) of $\Psi_Q(x,y)$ is negative, showing that $\Delta\varepsilon_Q < 0$. A pair of cross peaks which composed of a positive peak and a negative peak with different absolute intensities appears in domain I of the $\Psi_P(x,y)$ and the intensity of the positive peak on the right is stronger, which means $\Delta\varepsilon_P > 0$. The above analysis is proved to be correct by the spectral parameters for P, Q, U, and V used for the simulation listed in Table 7.

Table 7. Spectral Parameters of P, Q, U, and V in the Model System Where the Spectral Parameters of P and Q Undergo Complex Changes

spectral variable	peak position (cm^{-1})	bandwidth (cm^{-1})	absorptivity
P	150	20	1.0
Q	350	20	1.0
U	155	20	1.1
V	350	25	0.9

5. Example for Application of the DAOSD Method in a Real System. The interaction between benzene and iodine has been a chemical and physical curiosity for over sixty years.[52−58] The contributions of polarization, electrostatics, and dispersion are responsible for the stability of the iodine−benzene complex. Ab initio calculations were performed and showed that dispersion was the most important factor.[57,58] Thus, we select benzene−iodine/CCl_4 as a real chemical system to test the applicability of the DAOSD approach.

From spectral requirement point of view, the benzene−iodine/CCl_4 system is suitable for the DAOSD approach. This is manifested as follows:

(1) The characteristic peaks of the two solutes used in the DAOSD method should not overlap. Benzene shows a characteristic peak around 1813.2 cm^{-1}, which belongs to

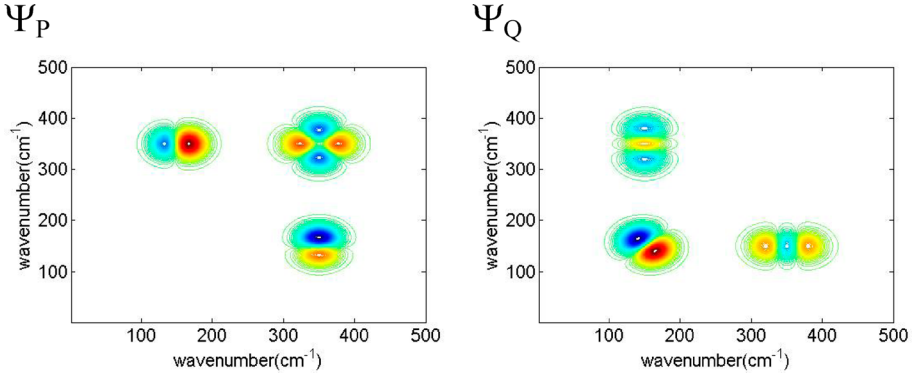

Figure 5. 2D asynchronous spectra generated by using the DAOSD approach on a model system where the spectral parameters of P and Q undergo complex changes.

dx.doi.org/10.1021/jp300918g | J. Phys. Chem. A 2012, 116, 10904−10916

its overtone band, whereas iodine has no absorbance above 1000 cm^{-1} in FT-IR spectra. Iodine has a characteristic peak around 517 nm corresponding to the electronic transition from $B^3\Pi_{ou}^+$ to $X^1\Sigma_g^+$ in UV−Vis spectra. Additionally, benzene does not show any absorbance i n the 400−700 nm region. Therefore, the overlapping problem of the characteristic peaks of two solutes is avoided.

(2) The absorption peaks of solvent do not overlap with the two characteristic peaks mentioned above. In UV−Vis spectra, CCl_4 have no absorbance in the 400−700 nm region. Similarly, no absorption band appears between 1900 and 1600 cm^{-1} in the FTIR spectrum of CCl_4. Thus, this requirement is also satisfied.

(3) The concentration should be adjusted to make sure it fits the Lambert−Beer law. CCl_4 solutions with only iodine or benzene as a solute were prepared. Good linearity is observed between absorbance and concentration when either iodine or benzene alone is dissolved in CCl_4 (Figures S3 and S4, Supporting Information), thereby excluding the possibility that the cross peaks are caused by solute−solvent interactions.[32,33]

In the experiment, two groups of solutions are prepared and each group contains four solutions. The concentration of benzene and iodine are designed according to the following rules: In the Group 1 solutions, the concentrations of benzene are invariant and the concentrations of iodine are set randomly. Similarly, the concentrations of iodine are invariant while the concentrations of benzene are set randomly in the Group 2 solutions. The concentrations of benzene and iodine in the two groups of solutions are within a region where the Lambert−Beer's law is valid. On the basis of the above rules, the concentrations of iodine and benzene in the two groups of solutions are summarized in Table 8. UV−Vis spectra and FT-IR spectra of the eight solutions are shown in Figure 6. The resultant 2D spectra are plotted in Figure 7.

Table 8. Initial Concentrations of Iodine and Benzene in CCl_4 Solutions That Meet the Requirement of the DAOSD Approach

index of the solutions	concn of benzene (v/v %)	concn of iodine (mg/mL)
	Group 1	
1	12.00	12.00
2	12.00	10.00
3	12.00	8.00
4	12.00	0.00
	Group 2	
1	12.00	8.00
2	10.00	8.00
3	6.00	8.00
4	0.00	8.00

A pair of strong cross peaks that are antisymmetric about the diagonal appears in domain II of asynchronous spectrum $\Psi_{benzene}$. The peak on the left is positive, which illustrates that the characteristic peak of iodine undergoes a blue shift upon intermolecular interactions. The negative cross peak is located at (535, 485) and the positive one is located at (485, 535). On the basis of the properties of peak position variation (Figure S2 in the Supporting Information), ΔX_{iodine} could be calculated as

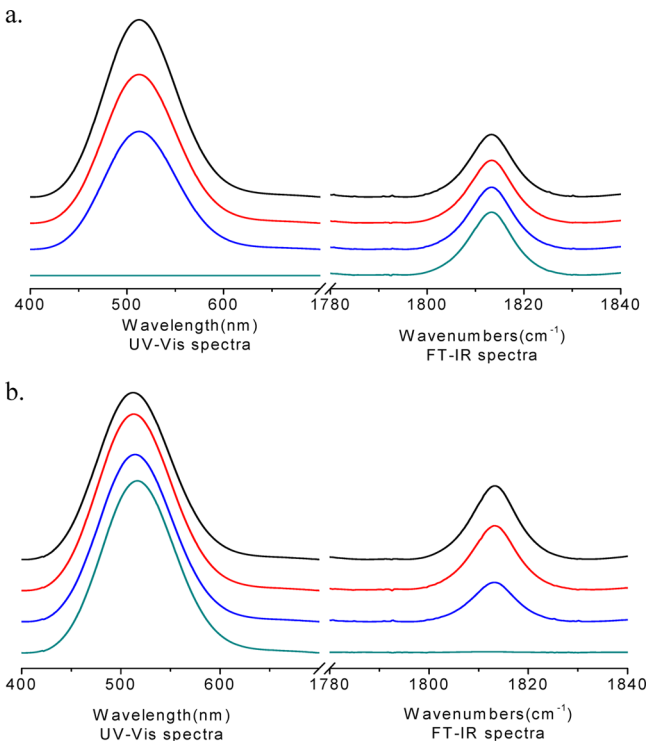

Figure 6. 1D UV−Vis spectra and FT-IR spectra of the iodine−benzene/CCl_4 solutions for generating 2D asynchronous spectra by using the DAOSD approach: (a) Group 1; (b) Group 2.

485 + 535 − 2 × 517 = −14 nm. As a result, we can estimate that the peak of iodine underwent a blue shift to 503 nm, which almost fit the result in the literature.[52] (The characteristic peak of iodine/benzene solute was located at 500 nm. The calculated result is not exactly the same because the concentration of benzene is much lower, so the environment around iodine in this system is different from iodine/benzene solution.) In addition, a pair of horizontal cross peaks (cross peak in the left is positive and peak in the left is negative) appears in domain I in Ψ_{iodine}, which also means the characteristic peak of iodine undergoes a blue shift. Moreover, the absolute value of the positive peak is slightly larger, which illustrates that the absorptivity of iodine increases.

A pair of cross peaks that are antisymmetric about the diagonal appears in domain III in Ψ_{iodine}. The peak on the left is positive, which illustrates that the characteristic peak of benzene undergoes a red shift upon intermolecular interactions. The negative cross peak is located at (1815.2, 1809.7) and the positive one is located at (1809.7, 1815.2). On the basis of the properties of peak position variation (Figure S2 in the Supporting Information), $\Delta X_{benzene}$ could be calculated as 1815.2 + 1809.7 − 2 × 1813.2 = −1.5 cm^{-1}. As a result, we can estimate that the peak of benzene blue-shifted to 1811.7 cm^{-1}. In addition, a negative cross peak appears in domain IV in $\Psi_{benzene}$, which also means the absorptivity of the characteristic peak of benzene decreases. The variation of peak position is quite weak, so the spectral patterns reflecting the variation of peak position is masked by the peak due to the variation of absorptivity.

In summary, the characteristic peak of iodine undergoes a large blue shift, which reflects the variation of the relative energy level of $B^3\Pi_{ou}^+$ and $X^1\Sigma_g^+$ states. The absorptivity of iodine slightly increases and that of benzene decreases which

dx.doi.org/10.1021/jp300918g | J. Phys. Chem. A 2012, 116, 10904−10916

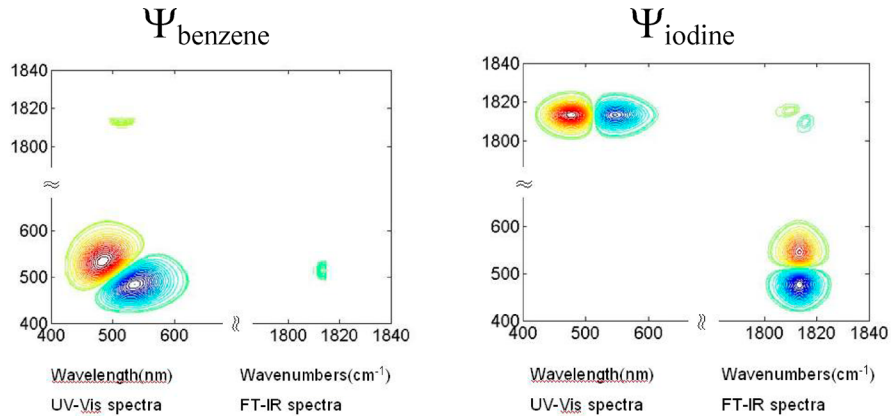

Figure 7. 2D asynchronous spectra according to the UV−Vis spectra and IR spectra of the iodine−benzene/CCl_4 system generated by using the DAOSD approach.

may reflect the variation of dipole moment of iodine and benzene in different fashions. Dipole−π electron interaction brings about a slight red shift of the overtone band of benzene.

CONCLUSION

A new approach called double asynchronous orthogonal sample design (DAOSD) is developed. A pair of complementary sub-2D asynchronous spectra is generated by using the DAOSD approach. Both theoretical analysis and computation simulation demonstrate that spectral variations of characteristic peaks of different solutes are manifested by cross peaks in separated regions in $\Psi_P(x,y)$ and $\Psi_Q(x,y)$. Thus, the 2D asynchronous spectra are much simplified by DAOSD approach, which facilitate the analysis of subtle spectral variations of characteristic peaks of substance under intermolecular interactions. Variations on peak position, bandwidth, and absorptivity can be estimated by the characteristic spectral pattern of cross peak in the pair of complementary sub-2D asynchronous spectra. The applicability of the DAOSD approach in the real chemical system has also been proved by an iodine−benzene/CCl_4 system. Therefore, the DAOSD approach can reveal subtle spectral variations, which is helpful to enhance our understanding on the nature of intermolecular interactions.

ASSOCIATED CONTENT

Supporting Information

The relationship between spectral patterns and $\Delta\varepsilon_Q$, ΔW_Q, and ΔX_Q is investigated comprehensively as an instance (the relationship between spectral patterns and $\Delta\varepsilon_P$, ΔW_P, and ΔX_P is similar). A one-to-one correspondence is established between the spectral patterns in $\Psi_P(x,y)$ and $\Psi_Q(x,y)$ and the types of variations of the peak position, bandwidth, and absorptivity of Q. Descriptions are provided on the spectral patterns of $\Psi_P(x,y)$ and $\Psi_Q(x,y)$ when $\Delta\varepsilon_Q$, ΔW_Q, and ΔX_Q change. Figures S1 and S2 show how to determine ΔW_Q and ΔX_Q from the spectral pattern from $\Psi_P(x,y)$ and $\Psi_Q(x,y)$. Texts are given on the UV−Vis spectra and FT-IR spectra of iodine/CCl_4 solutions and benzene/CCl_4 solutions, respectively. Figure S3 shows the relationship between the concentrations of iodine and the absorbance of corresponding characteristic peaks in UV−Vis spectra, and Figure S4 shows the relationships between the concentrations of benzene and the absorbance of corresponding characteristic peaks in FT-IR spectra. Good linearity is observed between absorbance and concentration when either iodine or benzene alone is dissolved in CCl_4. Complete refs 18, 22, 35, and 36. All the material is available free of charge via the Internet at http://pubs.acs.org.

AUTHOR INFORMATION

Corresponding Author

*E-mail: Y.X., xyz@pku.edu.cn; L.Y., yanglm@pku.edu.cn.

Notes

The authors declare no competing financial interest.

ACKNOWLEDGMENTS

The financial support from the National Natural Science Foundation of China (Grant No. 50673005, 50973003, 21136009, 51074150 and 21001009) and 973 Project (No. 2012CBA01203), National High-tech R&D Program of China (863 Program) of MOST (No. 2010AA03A406) is gratefully acknowledged.

REFERENCES

(1) Noda, I. *J. Am. Chem. Soc.* **1989**, *111*, 8116−8118.
(2) Noda, I. *Appl. Spectrosc.* **1990**, *44*, 550−561.
(3) Noda, I. *Appl. Spectrosc.* **1993**, *47*, 1329−1336.
(4) Noda, I. *Appl. Spectrosc.* **2000**, *54*, 994−999.
(5) Sasic, S.; Muszynski, A.; Ozaki, Y. *J. Phys. Chem. A* **2000**, *104*, 6380−6387.
(6) Thomas, M.; Richardson, H. H. *Vibr. Spectrosc.* **2000**, *24*, 137−146.
(7) Wu, Y. Q.; Jiang, J. H.; Ozaki, Y. *J. Phys. Chem. A* **2002**, *106*, 2422−2429.
(8) Wu, Y. Q.; Noda, I.; Meersman, F.; Ozaki, Y. *J. Mol. Struct.* **2006**, *799*, 121−127.
(9) Noda, I. *J. Mol. Struct.* **2006**, *799*, 34−40.
(10) Wu, Y. Q.; Noda, I. *Appl. Spectrosc.* **2006**, *60*, 605−610.
(11) Morita, S.; Shinzawa, H.; Noda, I.; Ozaki, Y. *Appl. Spectrosc.* **2006**, *60*, 398−406.
(12) Shinzawa, H.; Awa, K.; Okumura, T.; Morita, S.; Otsuka, M.; Ozaki, Y.; Sato, H. *Vibr. Spectrosc.* **2009**, *51*, 125−131.
(13) Padermshoke, A.; Sato, H.; Katsumoto, Y.; Ekgasit, S.; Noda, I.; Ozaki, Y. *Polymer* **2004**, *45*, 7159−7165.
(14) Zimmermann, B.; Baranovic, G. *Vibr. Spectrosc.* **2006**, *41*, 126−135.
(15) Yu, J.; Wu, P. Y. *Polymer* **2007**, *48*, 3477−3485.
(16) Choi, H. C.; Ryu, S. R.; Ji, H.; Kim, S. B.; Noda, I.; Jung, Y. M. *J. Phys. Chem. B* **2010**, *114*, 10979−10985.
(17) Heo, K. Y.; Yoon, J. W.; Jin, K. S.; Jin, S. W.; Sato, H.; Ozaki, Y. H.; Satkowski, M. M.; Noda, I.; Ree, M. *J. Phys. Chem. B* **2008**, *112*, 4571−4582.

(18) Sato, H.; Mori, K.; Murakami, R.; Ando, Y.; Takahashi, I.; Zhang, J. M.; Terauchi, H.; Hirose, F.; Senda, K.; Tashiro, K.; et al. *Macromolecules* **2006**, *39*, 1525−1531.
(19) Ausili, A.; Scire, A.; Damiani, E.; Zolese, G.; Bertoli, E.; Tanfani, F. *Biochemistry* **2005**, *44*, 15997−16006.
(20) Wang, G. F.; Gao, Y.; Geng, M. L. *J. Phys. Chem. B* **2006**, *110*, 8506−8512.
(21) Lefevre, T.; Arseneault, K.; Pezolet, M. *Biopolymers* **2004**, *73*, 705−715.
(22) Wang, L. X.; Wu, Y. Q.; Meersman, F. *Vibr. Spectrosc.* **2006**, *42*, 201−205.
(23) Yan, Y. B.; Zhang, J.; He, H. W.; Zhou, H. M. *Biophys. J.* **2006**, *90*, 2525−2533.
(24) Zhang, M.; Zhang, L. P.; Wu, Y. Q. *Vibr. Spectrosc.* **2011**, *57*, 319−325.
(25) Siuda, R.; Balcerowska, G.; Sadowski, C. *Food Addit. Contam.* **2006**, *23*, 1201−1207.
(26) Chen, Y. H.; Tian, H. L.; Li, J. H.; Li, G. Y. *Spectrosc. Spectral Anal.* **2012**, *32*, 1500−1506.
(27) Ren, G. D.; Guo, A. L.; Geng, F.; Ma, M. H.; Huang, Q.; Wu, X. F. *Spectrosc. Spectral Anal.* **2012**, *32*, 1780−1784.
(28) Dathe, H.; Haider, P.; Jentys, A.; Lercher, J. A. *J. Phys. Chem. B* **2006**, *110*, 26024−26032.
(29) Huang, J. Y.; Shih, W. T. *J. Phys.: Condens. Matter* **2006**, *18*, 7593−7603.
(30) Szyc, L.; Guo, J.; Yang, M.; Dreyer, J.; Tolstoy, P. M.; Nibbering, E. T. J.; Czarnik-Matusewicz, B.; Elsaesser, T.; Limbach, H. H. *J. Phys. Chem. A* **2010**, *114*, 7749−7760.
(31) Yu, Z. W.; Noda, I. *Appl. Spectrosc.* **2003**, *57*, 164−167.
(32) Qi, J.; Huang, K.; Gao, X. X.; Li, H. Z.; Liu, S. X.; Zhao, Y.; Xu, Y. Z.; Wu, J. G.; Noda, I. *J. Mol. Struct.* **2008**, *883*, 116−123.
(33) Qi, J.; Li, H. Z.; Huang, K.; Chen, H. H.; Liu, S. X.; Yang, L. M.; Zhao, Y.; Zhang, C. F.; Li, W. H.; Wu, J. G.; et al. *Appl. Spectrosc.* **2007**, *61*, 1359−1365.
(34) Chen, J.; Zhang, C.; Li, H.; Liu, Y.; Li, W.; Xu, Y.; Wu, J.; Noda, I. *J. Mol. Struct.* **2008**, *883*, 129−136.
(35) Zhang, C. F.; Huang, K.; Li, H. Z.; Chen, J.; Liu, S. X.; Zhao, Y.; Wang, D. J.; Xu, Y. Z.; Wu, J. G.; Noda, I.; et al. *J. Phys. Chem. A* **2009**, *113*, 12142−12156.
(36) Li, X. P.; Pan, Q. H.; Chen, J.; Liu, S. X.; He, A. Q.; Liu, C. G.; Wei, Y. J.; Huang, K.; Yang, L. M.; Feng, J.; et al. *Appl. Spectrosc.* **2011**, *65*, 901−917.
(37) Awichi, A.; Tee, E. M.; Srikanthan, G.; Zhao, W. *Appl. Spectrosc.* **2002**, *56*, 897−901.
(38) Tee, E. M.; Awichi, A.; Zhao, W. *J. Phys. Chem. A* **2002**, *106*, 6714−6719.
(39) Shinzawa, H.; Morita, S.; Awa, K.; Okada, M.; Noda, I.; Ozaki, Y.; Sato, H. *Appl. Spectrosc.* **2009**, *63*, 501−506.
(40) Czarnecki, M. A.; Czarnik-Matusewicz, B.; Ozaki, Y.; Iwahashi, M. *J. Phys. Chem. A* **2000**, *104*, 4906−4911.
(41) Sun, S. Q.; Li, C. W.; Wei, J. P.; Zhou, Q.; Noda, I. *J. Mol. Struct.* **2006**, *799*, 72−76.
(42) Liu, Y.; Zhang, G. J.; Sun, S. Q.; Noda, I. *J. Pharm. Biomed. Anal.* **2010**, *52*, 631−635.
(43) Wang, Y.; Xu, C. H.; Wang, P.; Sun, S. Q.; Chen, J. B.; Li, J.; Chen, T.; Wang, J. B. *Spectrochim. Acta A* **2011**, *83*, 265−270.
(44) Zhang, W.; Cao, Y. Z.; Liu, R.; Xu, K. X. *Spectrosc. Spectral Anal.* **2012**, *32*, 1507−1511.
(45) Mehl, G. H.; Goodby, J. W. *Angew. Chem., Int. Ed.* **1996**, *35*, 2641−2643.
(46) Sahu, K.; Roy, D.; Mondal, S. K.; Karmakar, R.; Bhattacharyya, K. *Chem. Phys. Lett.* **2005**, *404*, 341−345.
(47) Mandal, U.; Adhikari, A.; Dey, S.; Ghosh, S.; Mondal, S. K.; Bhattacharyya, K. *J. Phys. Chem. B* **2007**, *111*, 5896−5902.
(48) Dey, S.; Adhikari, A.; Mandal, U.; Ghosh, S.; Bhattacharyya, K. *J. Phys. Chem. B* **2008**, *112*, 5020−5026.
(49) Tschierske, C. *Angew. Chem., Int. Ed.* **2000**, *39*, 2454−2458.
(50) Nakash, M.; Goldvaser, M. *J. Am. Chem. Soc.* **2004**, *126*, 3436−3437.
(51) Iwahashi, M.; Suzuki, M.; Katayama, N.; Matsuzawa, H.; Czarnechki., M. A.; Ozaki, Y.; Wakisaka, A. *Appl. Spectrosc.* **2000**, *54*, 268−276.
(52) Benesi, H. A.; Hildebrand, J. H. *J. Am. Chem. Soc.* **1949**, *71*, 2703−2707.
(53) Fredin, L.; Nelander, B. *J. Am. Chem. Soc.* **1974**, *96*, 1672−1673.
(54) Grozema, F. C.; Zijlstra, R. W. J.; Swart, M.; Van Duijnen, P. Th. *Int. J. Quantum Chem.* **1999**, *75*, 709−723.
(55) Kiviniemi, T.; Hulkko, E.; Kiljunen, T.; Pettersson, M. *J. Phys. Chem. A* **2008**, *112*, 5025−5027.
(56) Weng, K.-F.; Shi, Y.; Zheng, X.; Phillips, D. L. *J. Phys. Chem. A* **2006**, *110*, 851−860.
(57) Mantione, M.-J. *Theo Chim Acta* **1968**, *11*, 119−127.
(58) Hanna, M. W.; Lippert, J. In *Molecular Complexes*; Foster, R., Eds.; Elek Science: London, 1973.